# Supplementary tables and figures

For "Lung cancer recurrence risk prediction through integrated deep learning evaluation" by

**Peng Huang [1,2,3,*], Peter B. Illei [3,4], Wilbur Franklin [5], Pei-Hsun Wu [6,7,8], Patrick M. Forde [1,3,9], Saeed Ashrafinia [10,11], Chen Hu [1,2,3], Hamza Khan [12], Harshna V. Vadvala [10], Ie-Ming Shih [3,4], Richard J. Battafarano [3,12], Michael A. Jacobs [3,10,13], Xiangrong Kong [2,14], Justine Lewis [15], Rongkai Yan [10], Yun Chen [16], Franck Housseau [1,3,9], Arman Rahmim [10,11,17], Elliot K. Fishman [1,3,10,12], David S. Ettinger [1,3], Kenneth J. Pienta [1,3], Denis Wirtz [1,3,6,7,8], Malcolm V. Brock [3,12], Stephen Lam [17,†] and Edward Gabrielson [3,4,†]**

**Table S1.** Surgical tissue histopathological features and clinical variables extracted from National Lung Screening Trial (NLST) database.

| Feature category | Features |
|---|---|
| Clinical measure | Lesion size (mm) in resected lung specimen,<br>Surgery type= (Sublobar resection; lobectomy)<br>Residual disease after the surgery (R0, R1)<br>Lymphadenectomy |
| Tumor regions | Regional highest tumor grade<br>Regional lymphoid infiltration<br>Regional vessel invasion<br>Highest regional tumor cell percent<br>Highest regional inflammatory cell percent<br>AIS = ("AIS Mixed Non-mucinous/Mucinous"; "AIS Mucinous"; "AIS Non-mucinous"; "AIS NOS or Indeterminate")<br>Adenocarcinoma = ("Solid Adenocarcinoma with mucin production"; "Solid Adenocarcinoma with mucin production; Clear Cell and Acinar"; "Acinar Adenocarcinoma"; "Adenocarcinoma Micropapillary"; "Adenocarcinoma, Mixed Subtype"; "Adenocarcinoma, NOS"; "Adenosquamous Carcinoma"; "Fetal Adenocarcinoma"; "Mucinous colloid carcinoma"; "Mucinous cystadenocarcinoma"; "Papillary Adenocarcinoma")<br>Carcinoid = ("Carcinoid Tumor; Atypical"; "Carcinoid Tumor, Typical"; "Carcinoid tumorlet")<br>Large Cell = ("Carcinoma NOS"; "Giant Cell Carcinoma"; "Large Cell Carcinoma"; "Large Cell Carcinoma with Rhabdoid Phenotype"; "Spindle Cell carcinoma")<br>Squamous = ("Squamous Cell Carcinoma"; "Squamous Cell Carcinoma, Basaloid"; "Squamous Cell Carcinoma, Clear Cell"; "Squamous Cell Carcinoma, Papillary") |
| Non-tumor regions | Chronic bronchitis<br>Emphysema<br>Fibrosis<br>Granuloma<br>Hemorrhage<br>Infarction<br>Necrosis<br>Pneumonia |
| Pre-malignant regions | "Squamous Dysplasia, MODERATE";<br>"Squamous dysplasia, SEVERE";<br>"Squamous Cell Carcinoma In Situ";<br>“None” |

**Table S2.** Radiomics and other texture features extracted from pre-operative low-dose CT screening images. Radiomics features were calculated using formulas from Aerts et al [21].

| Feature category | Features |
|---|---|
| First order statistics from within and peri-nodule regions | mean, median, variance, quantiles, skewness, kurtosis, energy, entropy, root mean square, uniformity. |
| Shape and volume from within and peri-nodule regions | compactness, maximum 3D diameter, sphericity, surface area, volume, surface to volume ratio |
| Gray level co-occurrence matrix (GLCM) texture features from within and peri-nodule regions | Autocorrelation, cluster prominence, cluster shade, cluster tendency, contrast, correlation, difference entropy, dissimilarity, energy, entropy, homogeneity 1 and 2, information measure of correlation 1 and 2, inverse difference moment normalized, inverse difference normalized, inverse variance, maximum probability, sum average, sum entropy, sum variance, variance. |
| Gray level run-length matrix (GLRLM) texture features from within and peri-nodule regions | Short run emphasis, long run emphasis, gray level non-uniformity, run length non-uniformity, run percentage, low gray level run emphasis, high gray run emphasis, short run low gray level emphasis, short run high gray level emphasis, long run low gray level emphasis, long run high gray level emphasis. |
| Contrast from within and peri-nodule regions | Ratios of mean intensities and quantiles between voxels inside the tumor and voxels in peri-tumor area |
| Voxel intensity spatial distribution from within the nodule | $LocSd_{100}$, $LocSdV_{100}$, $LocSd_{50}$, $LocSdV_{50}$, $LocSd_{20}$, $LocSdV_{20}$, $d_{50}$, $d_{20}$ |
| Tumor and other lesion location | RUL, RML, RLL, LUL, Lingular, LLL, carina, left hilum, right hilum, left main stem bronchus, right main stem bronchus, mediastinum, others |
| Emphysema | Lung median density and a binary indicator from the NLST data |
| Cardiovascular abnormality | A binary indicator from the NLST data |

**Figure S1**. Decoding synergy among input features within the deep learning black-box (A) and heatmap from top features inside the IDLE black-box (B).

A

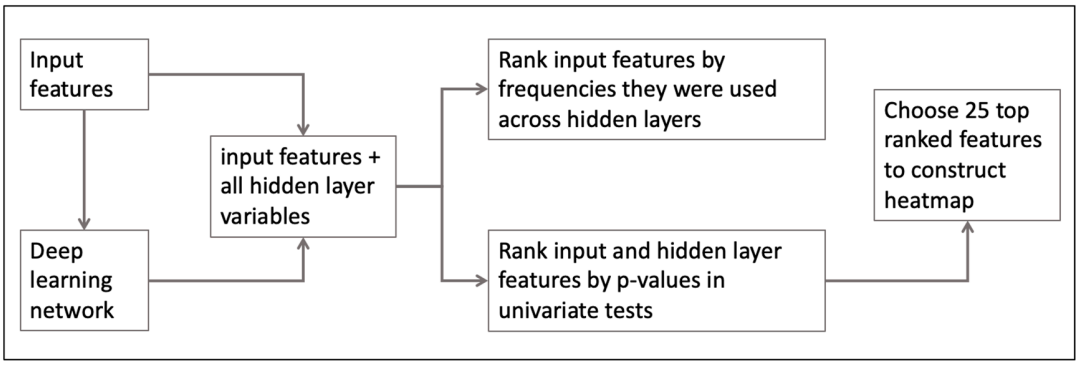


B

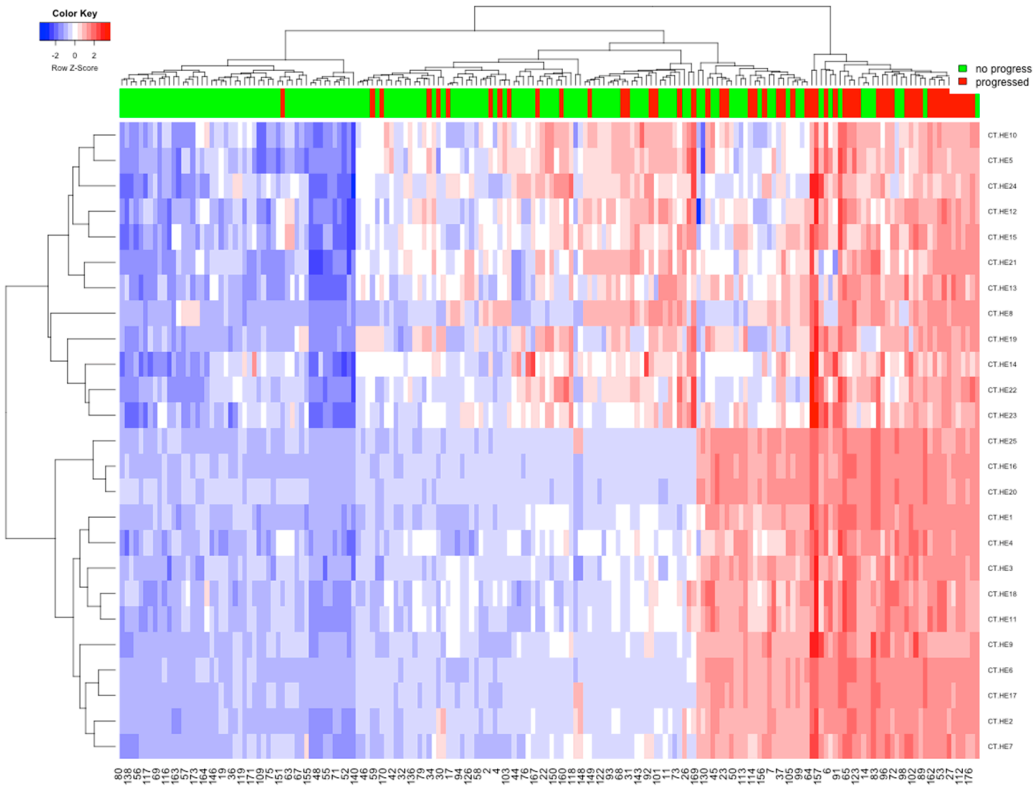
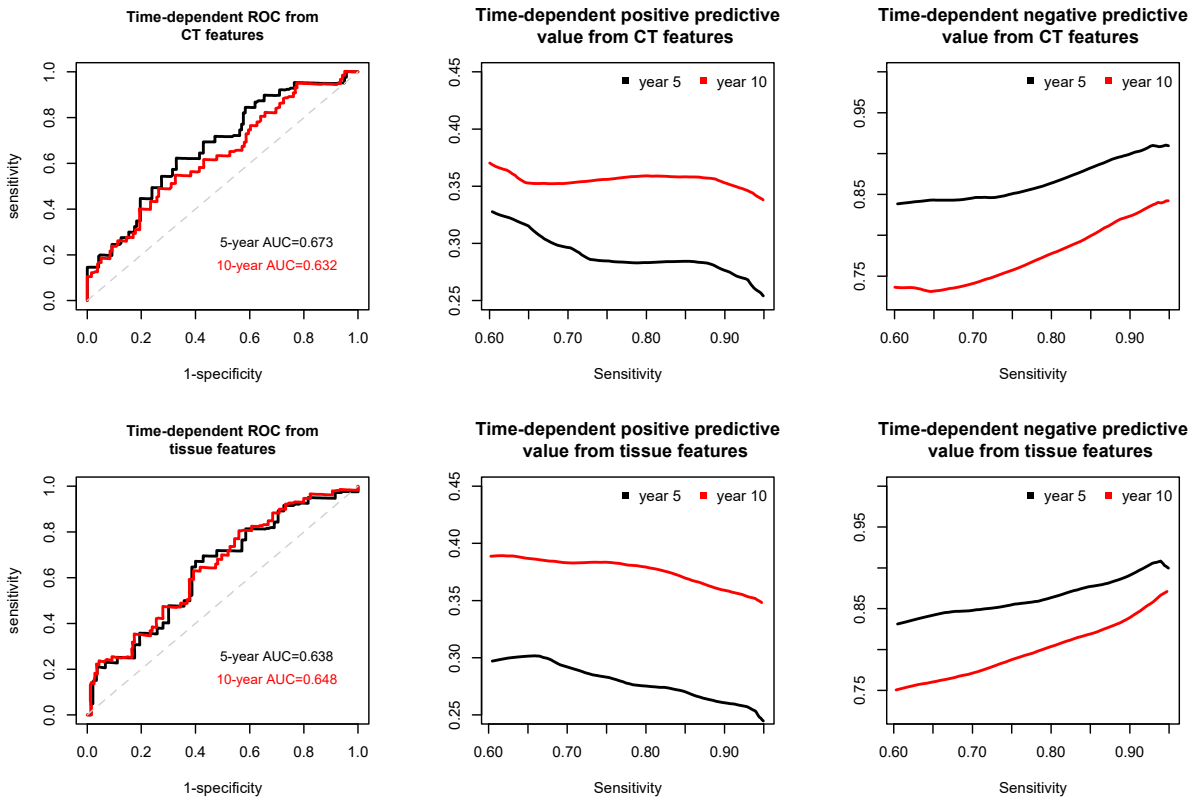
**Figure S2**. Prediction accuracies from pre-operative low-dose CT (LDCT) image feature-predicted scores (by excluding H&E features from the IDLE) and H&E feature-predicted scores (by excluding LDCT features from the IDLE). The method used to calculate these scores is the same as the method used to calculate IDLE scores, i.e., using leave-one-patient-out cross-validation.